Aeroheating Measurements of BOLT Aerodynamic Fairings and Transition Module

Elizabeth F. Rieken*, Scott A. Berry†, Casey J. Broslawski‡,and Francis A. Greene§
NASA Langley Research Center, Hampton, VA 23681

The Air Force Office of Scientific Research (AFOSR) has sponsored the Boundary Layer Transition (BOLT) Experiments to investigate hypersonic boundary layer transition on a low-curvature, concave surface with swept leading edges. This paper presents aeroheating measurements on a subscale model of the BOLT Flight Geometry, aerodynamic fairings, and Transition Module (TSM) in the NASA Langley 20-Inch Mach 6 Air Tunnel. The purpose of the test was to investigate and identify any areas of localized heating on the TSM for inclusion in the BOLT Critical Design Review (CDR). Surface heating distributions were measured using global phosphor thermography, and data were obtained for a range of model attitudes and free stream Reynolds numbers. Measurements showed low heating on the fairings and TSM. Additional analysis was completed after the CDR to compare heating on the TSM for the nominal BOLT vehicle reentry angle-of-attack with heating on the TSM for possible reentry angle-of-attack excursions. The results of this analysis were used in conjunction with thermal analyses from Johns Hopkins Applied Physics Lab (JHU/APL) and the Air Force Research Laboratory (AFRL) to assess the need for thermal protection on the flight vehicle TSM.

I. Nomenclature

H_{AW}	=	adiabatic wall surface enthalpy, J/kg
H_W	=	surface enthalpy, J/kg
H_0	=	wind tunnel total enthalpy, J/kg
H_{300K}	=	enthalpy at 300 K temperature, J/kg
h	=	convective heat transfer coefficient, kg/(m^{2}s)
h_{FR}	=	convective heat transfer coefficient based on Fay-Riddell theory, kg/(m^{2}s)
M_∞	=	freestream Mach number
q	=	heat transfer rate, W/m^2
Re_L	=	length Reynolds number
Re_∞	=	freestream unit Reynolds number, 1/m
T_∞	=	freestream temperature, K
U_∞	=	freestream velocity, m/s
α	=	model angle-of-attack, deg
β	=	model yaw, deg
ρ_∞	=	freestream density, kg/m^3

II. Introduction

The Air Force Office of Scientific Research (AFOSR) has sponsored the Boundary Layer Transition (BOLT) Experiments with an objective to investigate hypersonic boundary layer transition mechanisms on a complex geometry. Johns Hopkins University Applied Physics Laboratory (JHU/APL) is overseeing the BOLT team, which includes members from government, academia, and industry. Progressing from the Hypersonic International Flight Research Experimentation Program (HIFiRE) axisymmetric circular cone (HIFiRE-1) and nonaxisymmetric elliptical cones

*Aerospace Engineer, Aerothermodynamics Branch, AIAA Member
†Aerospace Engineer, Aerothermodynamics Branch, AIAA Associate Fellow
‡Pathways Intern, Aerothermodynamics Branch, AIAA Student Member
§Aerospace Engineer, Aerothermodynamics Branch, AIAA Associate Fellow

(HIFiRE-5A/HIFiRE-5B), the BOLT geometry is a low-curvature, concave surface with swept leading edges. The BOLT Experiments are designed to use numerical prediction tools and ground-test campaigns to estimate transition on the BOLT geometry. The project will culminate in a sounding rocket flight experiment to test the prediction effort. Ref.[1] provides an overview of the BOLT flight experiment.

The BOLT sounding rocket flight experiment is made-up of the BOLT experimental payload, or "Flight Geometry," the Payload System, which includes systems to support data acquisition, telemetry, and GPS, and the Launch Vehicle System, which consists of a two-stage sounding rocket stack. Leading up to the BOLT Critical Design Review (CDR), there was a concern about the interface between the BOLT Flight Geometry and the Payload System. Aerodynamic fairings were deemed necessary to reduce flow separations and reattachments on the Payload System. Figure 1 shows the Flight Geometry attached to four fairings, the Transition Module (TSM) and Payload Support Module (PSM). The TSM and PSM are part of the Payload System of the flight vehicle. NASA Langley had previously run an aeroheating test of the BOLT Flight Geometry early on in the BOLT project to support initial flight experiment designs [2]. One month prior to the CDR, the team at NASA Langley received the final aerodynamic fairing design and ran a fast-paced wind tunnel test of a new model encompassing the BOLT Flight Geometry, fairings, and TSM, in order to investigate and identify any aeroheating issues on the fairings and TSM for inclusion in the CDR proceedings.

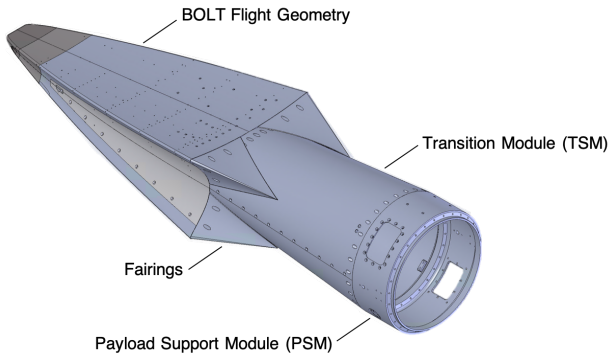

Fig. 1 BOLT Flight Geometry, aerodynamic fairings, TSM, and PSM

After the CDR, additional numerical modeling work was done by JHU/APL and the Air Force Research Laboratory (AFRL) to look at the complex flow field that the BOLT geometry creates on the fairings and TSM. JHU/APL completed a thermal analysis of the fairings and TSM in order to determine the need for thermal protection on these vehicle components. In the calculations, a 1.2 margin of safety was used on the heat transfer coefficient. Wind tunnel aeroheating data over a range of model attitudes were used to determine if the possible heating ranges for off-nominal flight vehicle reentry cases were encompassed by the 1.2 factor of safety.

This paper describes aeroheating measurements of the BOLT Flight Geometry, fairings, and TSM in the NASA Langley 20-Inch Mach 6 Air Tunnel. Global heating distributions are presented for the nominal BOLT flight experiment reentry angle-of-attack and for angle-of-attack excursions. Discussion and analysis focus on the fairings and TSM region of the model. Heating on the TSM for the nominal vehicle reentry angle-of-attack case is compared with heating for two off-nominal vehicle reentry cases.

III. Experimental Methods

A. Test Facility

The data in this paper were acquired in the NASA Langley 20-Inch Mach 6 Air Tunnel, which is part of the Langley Aerothermodynamics Laboratory (LAL) facilities [3]. The NASA LaRC 20-Inch Mach 6 Air Tunnel is a conventional hypersonic blowdown facility that uses heated, dried, and filtered air as the test gas. The maximum temperature achievable is 555.6 K and the nominal operating pressure range is from 206.8 kPa to 3275 kPa. A two-dimensional, contoured nozzle is used to provide perfect-gas freestream conditions with freestream Mach numbers of 5.8 to 6.1 and unit Reynolds numbers of 1.6×10^6/m (0.5×10^6/ft) to 27.2×10^6/m (8.3×10^6/ft). The nozzle throat is 8.64-mm by 508-mm (0.34-in by 20.0-in), which then expands into the 508-mm by 521-mm (20.0-in by 20.5-in) test section. A bottom-mounted model injection system is used to insert models from a sheltered position to the tunnel centerline, which

for these aeroheating tests was done as quickly as possible (less than 0.5-sec traverse through the tunnel boundary layer). Run times up to 20 minutes are possible with this facility, although for the current heat transfer tests, the model was exposed to the flow for only a few seconds. Flow conditions are typically determined, based on perfect-gas calculations, from the measured reservoir pressure and temperature and the measured pitot pressure at the test section.

B. Model

A ceramic wind tunnel model was fabricated using the process outlined in Ref. [4]. The model included the BOLT Flight Geometry, four fairings, and the TSM portion of the payload section. On the flight vehicle, the full scale BOLT Flight Geometry is 866-mm (34.1-in) long, the TSM is 561-mm (22.1-in) long, and the aerodynamic fairings are 246-mm (9.7-in) long. The wind tunnel model was a quarter-scale model with a 216-mm (8.52-in) long BOLT Flight Geometry, a 140-mm (5.52-in) long TSM, and 61.5-mm (2.42-in) long fairings. The total model length was 356-mm (14.03-in) long. The model coordinate system and reference dimensions used for analysis are shown in Fig. 2 . Figure 3 shows the model coated with phosphors, and installed in the retracted position of the 20-Inch Mach 6 Air Tunnel.

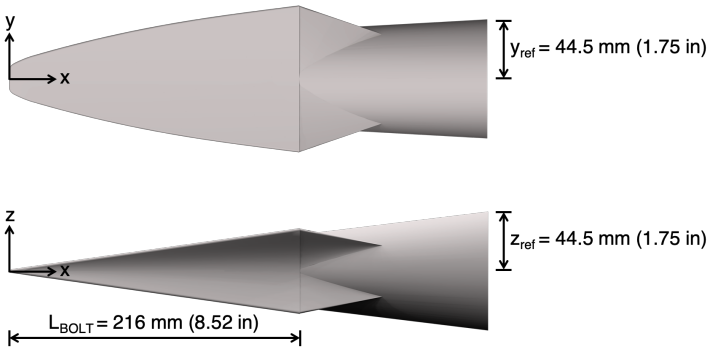

Fig. 2 Model coordinate system and reference dimensions.

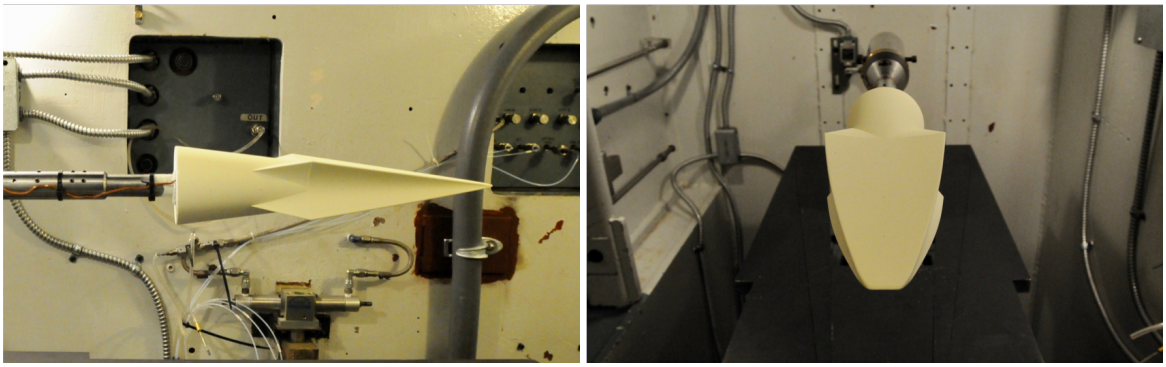

Fig. 3 Subscale BOLT model shown in the 20-Inch Mach 6 Air Tunnel in the retracted position.

C. Test Conditions

As discussed in Ref. [1], the Re_L expected in flight for BOLT during the test window of interest varies from 1×10^6 to 20×10^6. For the quarter-scale model where the reference length is based on the Flight Geometry length of 216 mm (8.52 in), the Re_L for this test varied from 1.4×10^6 to 5.6×10^6. The nominal reentry total angle-of-attack for BOLT is near 0°. However, combined angle-of-attack and yaw excursions are likely, with less than ±2° being the desired goal and ±5° being acceptable. The wind tunnel test matrices were set up to explore the impact of these excursions, in both pitch and yaw, in order to understand the possible aeroheating environments on the fairings and TSM for the nominal flight path and for nominal flight path excursions. In this work, the nominal reentry case refers to an $\alpha = 0°$ and $\beta = 0°$ model attitude.

In addition to varying the model attitude, the freestream Reynolds number and the model viewing orientation was changed. Freestream conditions for the Re_∞ values run during the test are listed in Table 1. The conditions are averaged values based on all runs at a given condition. The model was run at two different viewing orientations in order to get heating data on both the top and side surface of the model. The model was first run in the orientation shown in Fig. 3 to view the top surface of the model from the upper window of the test section. Next, the model was rotated 90° to view the side surface of the model from the upper window of the test section.

Table 1 20-Inch Mach 6 Air Tunnel Conditions.

Re_∞ (1/m)	Re_L	M_∞	T_∞ (K)	ρ_∞ (kg/m^3)	U_∞ (m/s)
6.69×10^6	1.45×10^6	5.96	62.9	3.18×10^{-2}	947.2
13.2×10^6	2.86×10^6	6.01	62.2	6.23×10^{-2}	948.0
26.1×10^6	5.65×10^6	6.03	60.1	1.21×10^{-1}	932.2

D. Phosphor Thermography Technique

1. Data Acquisition and Reduction

Aeroheating data were obtained using two-color, relative-intensity, global phosphor thermography and reduced using the Imaging for Hypersonic Experimental Aeroheating Testing (IHEAT) software. The global phosphor thermography method uses slip-cast ceramic wind tunnel models coated with a thermographic phosphor compound. The models are illuminated by an ultraviolet light source, producing a temperature-dependent fluorescence of the phosphor coating. A three-color charge-coupled device (CCD) camera is used to take images of the model fluorescence intensity before the wind tunnel run and during a wind tunnel run when the model is exposed to hypersonic flow. Details of the phosphor thermography technique are provided in Refs. [5, 6].

The IHEAT software uses a phosphor calibration to convert the intensity data from each image pixel to a temperature. Convective heat transfer coefficients are then determined using one-dimensional heat conduction theory assuming a step function in heat transfer beginning at the injection of the model into the tunnel. Heat transfer data from IHEAT are typically reported in terms of h/h_{FR}, where h_{FR} is the heat transfer film coefficient resulting from a Fay-Riddell computation for a reference hemisphere of a specified radius (in this case, a 0.05 in nose radius). Convective heat transfer coefficients are calculated from a convective heat transfer equation defined in terms of enthalpy as seen in Eq.(1):

$$h = q/(H_{AW} - H_W) = q/(H_0 - H_{300K}) \tag{1}$$

Details of the IHEAT software, including additional heat transfer calculation assumptions and equations are described in Refs. [5, 7].

2. Data Uncertainty

The experimental uncertainty for convective heat transfer measurements resulting from the phosphor thermography data acquisition and reduction method is typically between 8-10% as discussed in Ref. [5]. The phosphor data uncertainty is dependent on the rise in model surface temperature, resulting in higher uncertainty when the model surface temperature rise is low such as is the case for some regions of the model in this test. Based on the uncertainty analysis in Ref. [5] and historical tests with a variety of models, the data from the fairings and TSM regions of the BOLT model where the temperature rise is low (10-20 °C) have an uncertainty of roughly ±25% . Additional uncertainty is also due to tunnel flow quality, test-condition repeatability, and the two-dimensional mapping of image pixel location to the physical location on the model. Computational heating predictions for both a laminar and turbulent flow field were completed as a benchmark for the experimental data. As will be shown later, the predicted and measured heating distributions had good agreement.

E. Computational Method

The numerical results presented in this paper were computed using The Langley Aerothermodynamic Upwind Relaxation Algorithm (LAURA) [8, 9]. LAURA is a finite-volume shock-capturing structured-grid computational

fluid dynamics (CFD) tool specialized for hypersonic reentry flows. Either the Euler, thin-layer Navier-Stokes, or full Navier-Stokes equations are relaxed in pseudotime to a steady state. First-order inviscid fluxes are constructed using Roe's flux difference splitting with Harten's entropy fix and are extended to second-order using Yee's Symmetric Total Variational Diminishing (STVD) limiting. Second-order central differences approximate the viscous fluxes. LAURA can utilize point or line-implicit relaxation and employs MPI to run efficiently on parallel computing architectures.

Figure 4 shows results of a four-level mesh refinement study, with coarser grids constructed by removing every other surface point. Plotted is nondimensional heating (h/h_{FR}) along the vehicle centerline for each grid level, with the finest grid consisting of 744 blocks with 33 x 33 x 129 points in each block (98 million cells). The 129 points through the layer remained unchanged for all levels of mesh refinement. While the BOLT centerline appears grid-converged, changes in mesh resolution continue, to a small degree, to influence TSM heating. Percent changes in heating between fine and medium mesh values were less than 1% on the BOLT Fight Geometry and 10% on the TSM. The highest percent differences occur where the heating is lowest, so the absolute change in heating is quite small. The medium mesh results were used for experimental data comparison.

The outer domain of each solution grid is adapted to follow the contour of the bow shock. Points within the domain are clustered to resolve the flow in the boundary layer using an adaptation algorithm in LAURA. Along each line normal to the surface, this algorithm redistributes points such that a limited number (i.e., 5) remain in the freestream and the cell height spacing at the wall is based on a user-prescribed wall cell Reynolds number (0.50). Having a machine zero L2 error norm or a percentage change in heating of less than 0.1% over 5000 iterations defined convergence. Presented in the paper are laminar and turbulent (Cebeci-Smith, [10]) full Navier-Stokes solutions computed using a computational mesh containing approximately 25 million cells covering a quarter of the vehicle, including the TSM. The quarter geometry is appropriate given the vehicle symmetry and that all simulations are at a 0° angle-of-attack and yaw.

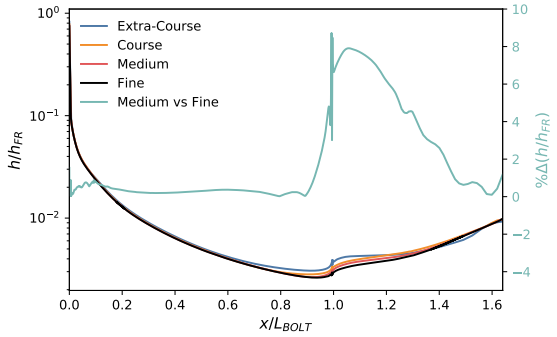

Fig. 4 Mesh refinement along model centerline for $Re_L = 1.4 \times 10^6$ at the nominal vehicle reentry attitude ($\alpha = 0°, \beta = 0°$).

IV. Results and Analysis

Global surface convective heating data were obtained from 49 runs for a range of angle-of-attack, yaw, and Reynolds number with a view of the top and side surface of the model. The goal of this test and the results and analysis included in this paper focus on the fairings and TSM regions of the model. Refs. [2, 11–13] provide ground test measurements and analysis of boundary layer transition and boundary layer instability on the BOLT Flight Geometry. In the present paper, a subset of the most relevant results on the fairing and TSM for the BOLT flight experiment are shown. First, global surface heating for the nominal vehicle reentry case ($\alpha = 0°$, $\beta = 0°$) is shown along with a comparison of wind tunnel heating data and computational predictions along the model centerline and at an aft axial station. Then, global surface heating for two off-nominal vehicle reentry cases are shown along with a comparative analysis of heating on the TSM for the different vehicle reentry cases.

A. Nominal Surface Heating Data

Figure 5 provides global heating distributions for three Re_L conditions at the nominal vehicle reentry case. Consistent with previous results in Ref. [2], there is a systematic movement of transition with increasing Re_L, evidenced by the development of two higher-heating lobes on either side of the model centerline. The focus of this analysis is on the

fairings and TSM regions of the model. A complex flow field aft of the BOLT Flight Geometry creates areas of localized heating on the TSM due to compression and shock boundary layer interactions. However, the peak heating values on the TSM are significantly lower than the peak heating values on the BOLT Flight Geometry. The fairings exhibit even lower heating than the TSM. Preliminary global heating distributions on the fairings and TSM were presented at the BOLT CDR four weeks after finalizing the model geometry.

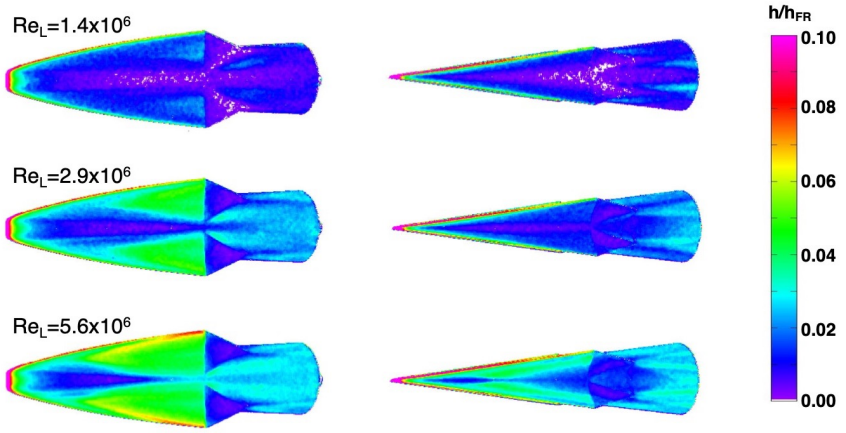

Fig. 5 Global heating distributions at the nominal vehicle reentry attitude ($\alpha = 0°$, $\beta = 0°$).

Figure 6 provides a comparison of extracted heating data from the nominal global heating distributions and CFD predictions. Figure 6(a) compares fully laminar and fully turbulent CFD predictions to the model centerline heating for three Re_L cases. The laminar CFD solution for the $Re_L = 1.4 \times 10^6$ case compares well to the wind tunnel heating data for the same condition and shows a slight offset in the laminar regions of the higher Re_L cases. The turbulent CFD solution for the $Re_L = 5.6 \times 10^6$ case shows good agreement with the wind tunnel heating data for the same condition after transition occurs. Figure 6(b) compares heating along an axial station just aft of the fairings on the TSM. The wind tunnel data and CFD predictions match reasonably well, although less closely than along the model centerline. Both the wind tunnel data and the CFD predictions show higher heating streaks on either side of the centerline. The streaks are more pronounced and have higher peak heating in the CFD computational predictions. Given the low model surface temperature rise and the simple two-dimensional method used to extract linecuts within IHEAT, the axial TSM CFD predictions and wind tunnel data show reasonable agreement. Overall these comparisons provide validation that the wind tunnel data are useful even with the higher uncertainty due to low model surface temperature rise on the TSM.

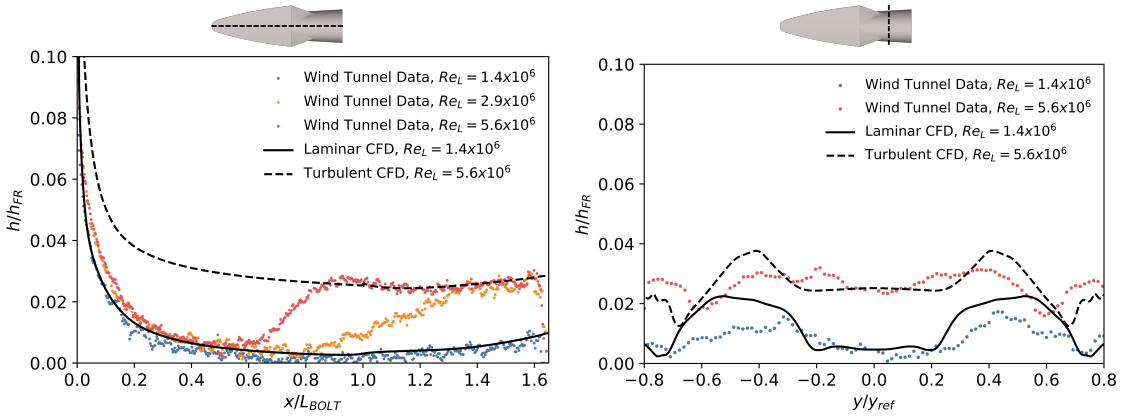

(a) Model centerline data.

(b) Axial data at x/L$_{BOLT}$=1.32.

Fig. 6 Comparison of heating data and CFD at the nominal vehicle reentry attitude ($\alpha = 0°$, $\beta = 0°$).

B. Off-Nominal Surface Heating Data

After the BOLT CDR, the BOLT team at JHU/APL completed a thermal analysis of the BOLT fairings and TSM. The purpose of this thermal analysis was to determine expected temperatures on the fairings and TSM and the potential need for thermal protection on these parts. The analysis was done for the nominal vehicle reentry angle-of-attack with several conservative assumptions, including a 1.2 factor of safety on the calculated heat transfer coefficient, which was in turn used to calculate the thermal response. The heating data from this test were used as a comparison point to see how the heating for an off-nominal total angle-of-attack excursion compared to heating for the nominal reentry angle-of-attack.

For the present analysis, two off-nominal cases were considered. The first was a 2° total angle-of-attack reentry case and the second was a 5° total angle-of-attack reentry case. The flight vehicle will be spin stabilized on reentry and therefore, will roll through various combinations of α and β for a set total angle-of-attack. In order to capture an average value for heating on the TSM during a roll cycle, four model attitudes were used in the analysis. For the 2° total angle-of-attack reentry case, model attitudes of (1) $\alpha = 2°$, $\beta = 0°$, (2) $\alpha = 0°$, $\beta = 2°$, (3) $\alpha = 0°$, $\beta = -2°$, and (4) $\alpha = -2°$, $\beta = 0°$ were considered. Similarly, for the 5° total angle-of-attack reentry case, model attitudes of (1) $\alpha = 5°$, $\beta = 0°$, (2) $\alpha = 0°$, $\beta = 5°$, (3) $\alpha = 0°$, $\beta = -5°$, and (4) $\alpha = -5°$, $\beta = 0°$ were considered.

Due to the symmetry of the BOLT geometry, the top surface $\pm\beta$ cases and the side surface $\pm\alpha$ cases are symmetric. To confirm that the wind tunnel heating data could be considered symmetric in these instances, a symmetry check was conducted for a $\beta = \pm 2°$ top surface view case. Figure 7 shows heating data extracted at an axial station at $x/L_{BOLT} = 1.32$ on the TSM for both $\alpha = 0°$, $\beta = 2°$ and $\alpha = 0°$, $\beta = -2°$ model attitudes. A symmetric reflection of the $\alpha = 0°$, $\beta = 2°$ data across the $y/y_{ref} = 0$ centerline shows good agreement with the $\alpha = 0°$, $\beta = -2°$ case. Symmetric reflection of the data was used for subsequent symmetric cases (e.g., the top surface $\alpha = 0°$, $\beta = -5°$ data are symmetric reflections of the top surface $\alpha = 0°$, $\beta = 5°$ data).

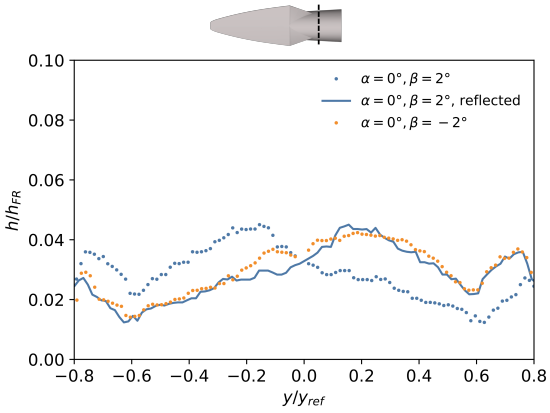

Fig. 7 Data symmetry confirmation for $\beta = \pm 2°$ at x/L$_{BOLT}$=1.32 for $Re_L = 5.6 \times 10^6$.

Global surface convective heating data for the 2° and 5° total angle-of-attack off-nominal reentry cases are shown in Figs. 8- 11. Figure 8 provides heating data for the 2° reentry case at $Re_L = 2.9 \times 10^6$. As expected, heating on the TSM is higher on the windward side of the vehicle compared to the leeward side of the vehicle (note that the view of the top surface of the model at a model attitude of $\alpha = -2°$ is the windward surface.) On the top surface, the $\beta = \pm 2°$ model attitudes show a change in heating pattern on the TSM as compared to the nominal case. In these yaw attitudes, the asymmetric transition fronts on the BOLT Flight Geometry result in higher heating on one side of the TSM. On the side surface, heating asymmetry occurs with $\alpha = \pm 2°$ resulting in stronger heating streaks on the windward side of the top surface. In all cases, heating on the fairings was very low.

Similar heating trends discussed in the above paragraph exist for all four reentry cases considered in this analysis. TSM heating increases with Re_L and with model angle-of-attack. Heating on the fairings is low for all model attitudes with some heating starting to develop in the $\alpha = -5°$, $\beta = 0°$ attitude on the forward portion of the fairing that is attached to the BOLT Flight Geometry. In all cases, peak heating on the TSM is lower than peak heating on the BOLT top surface.

To compare heating for an off-nominal total angle-of-attack excursion with heating for the nominal reentry angle-of-attack, heating data were extracted along two axial stations on the TSM as indicated in Figure 12. Station A was

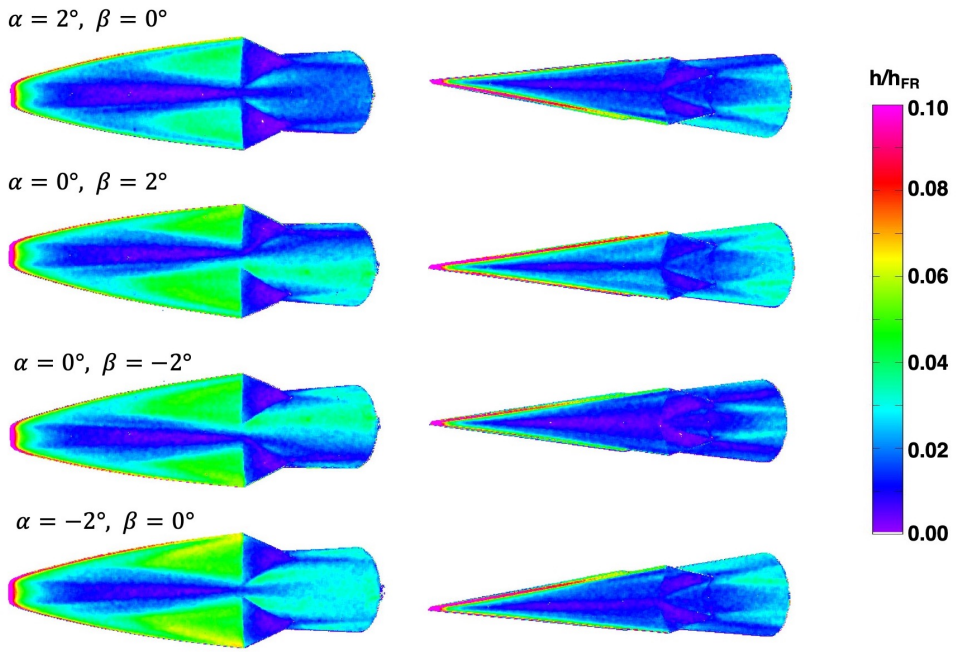

Fig. 8 Global heating distributions representing a 2° total angle-of-attack off-nominal vehicle reentry attitude for $Re_L = 2.9 \times 10^6$.

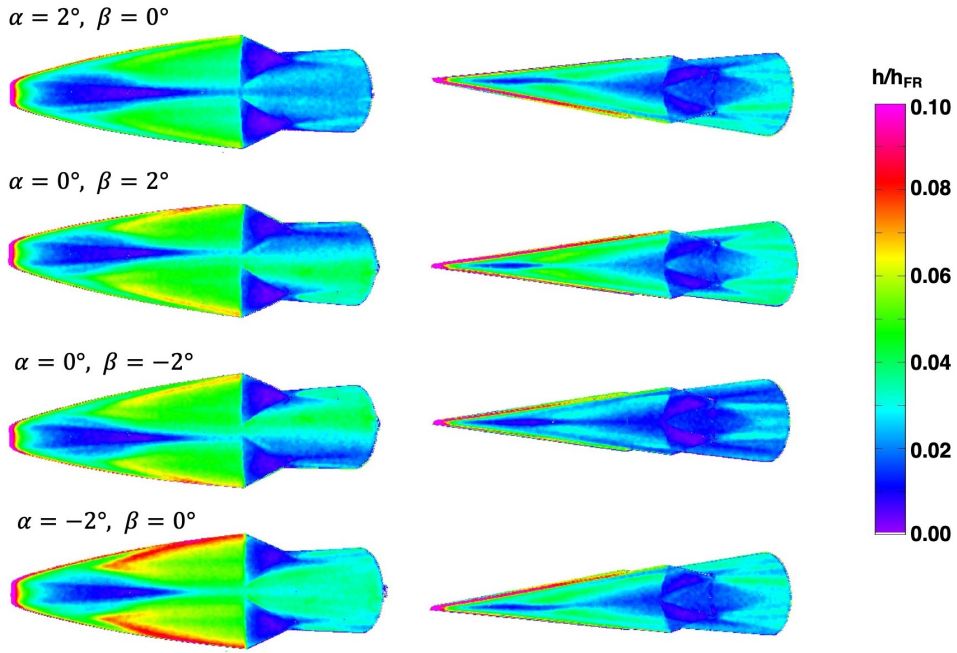

Fig. 9 Global heating distributions representing a 2° total angle-of-attack off-nominal vehicle reentry attitude for $Re_L = 5.6 \times 10^6$.

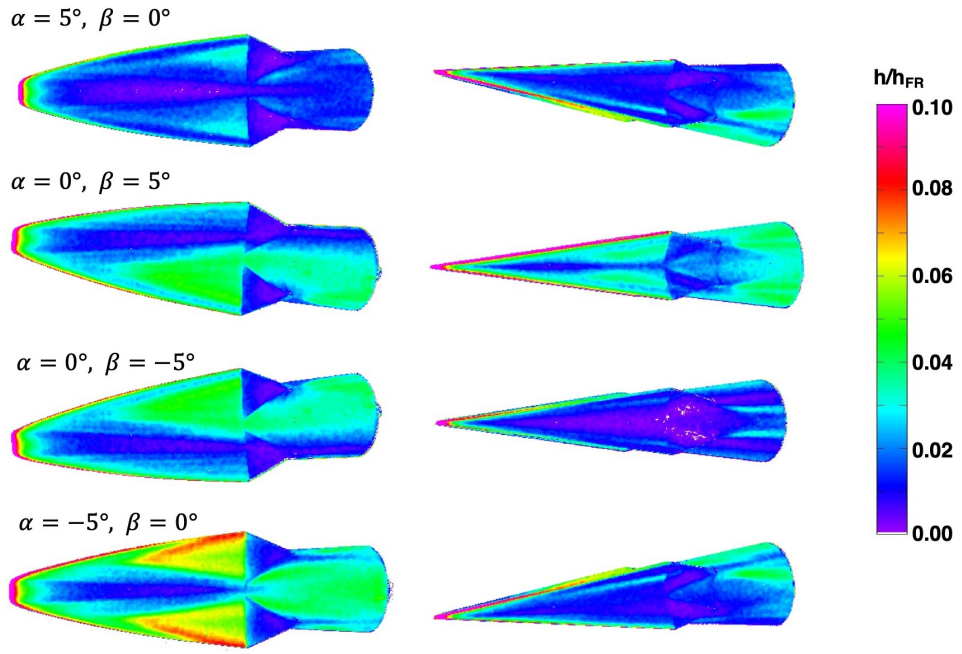

Fig. 10 Global heating distributions representing a 5° total angle-of-attack off-nominal vehicle reentry attitude for $Re_L = 2.9 \times 10^6$.

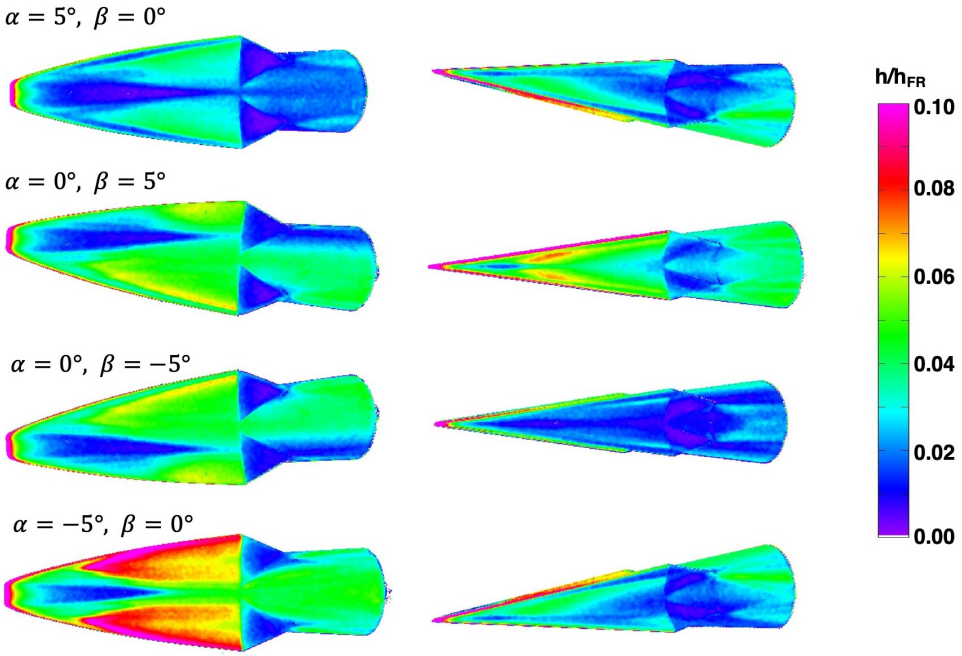

Fig. 11 Global heating distributions representing a 5° total angle-of-attack off-nominal vehicle reentry attitude for $Re_L = 5.6 \times 10^6$.

just beyond the fairing tips at $x/L_{BOLT} = 1.32$ and station B was further downstream on the TSM at $x/L_{BOLT} = 1.48$. Heating values at each station across the four model attitudes were averaged to represent average heating over a 2° or 5° roll cycle. An example is shown in Fig. 13; heating along the station A cut on the top surface is plotted for the four model attitudes considered for a 5° roll cycle. The black line shows the resulting average of the four cuts.

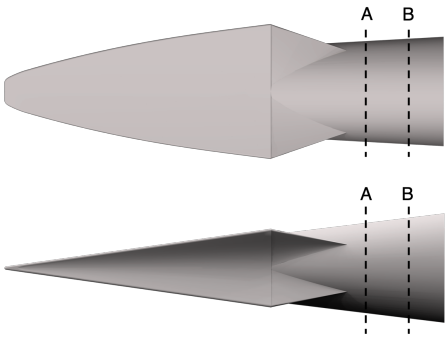

Fig. 12 TSM axial station locations.

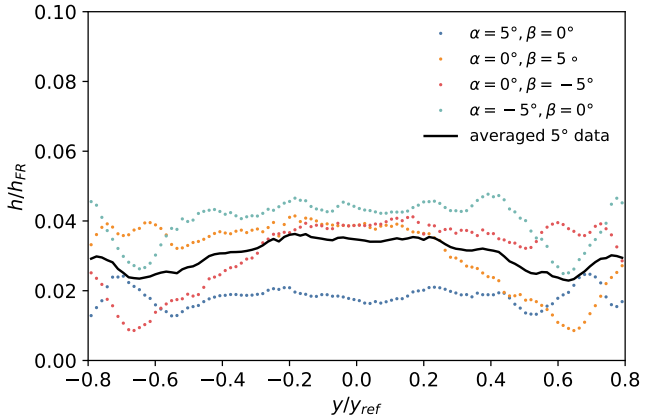

Fig. 13 Example average heating calculation on the top surface at station A for $Re_L = 5.6 \times 10^6$, representing a 5° total angle-of-attack vehicle reentry attitude.

The 2° and 5° averaged heating values for the top and side surfaces for $Re_L = 2.9 \times 10^6$ and $Re_L = 5.6 \times 10^6$ were plotted against the 0° heating at the corresponding axial station. Figure 14 provides heating comparisons for the $Re_L = 2.9 \times 10^6$ data and Fig. 15 provides heating comparisons for the $Re_L = 5.6 \times 10^6$ data. The off-nominal reentry averaged heating is generally higher than the 0° reentry heating. In order to quantitatively compare the off-nominal case to the nominal case, the maximum heating value for each case was used as this represents the peak heating to the TSM material. For example, using the data in Fig 15(a), the maximum heating value for the averaged 5°, top surface, $Re_L = 5.6 \times 10^6$ data was divided by the maximum heating for the 0°, top surface, $Re_L = 5.6 \times 10^6$ data to get a maximum heating ratio. This tabulation was done for each comparison case and the results are shown Table 2.

Table 2 Off-nominal to nominal reentry angle-of-attack heating ratios.

Angle	Surface	Re_L	Max Heat Ratio Station A	Max Heat Ratio Station B
2°	Top	2.9×10^6	1.09	1.03
2°	Side	2.9×10^6	1.06	0.94
5°	Top	2.9×10^6	1.12	1.08
5°	Side	2.9×10^6	1.11	0.96
2°	Top	5.6×10^6	1.08	1.13
2°	Side	5.6×10^6	1.03	0.93
5°	Top	5.6×10^6	1.15	1.19
5°	Side	5.6×10^6	1.08	0.96

The results in Table 2 show that for all cases considered in this analysis, the maximum heating value for the off-nominal reentry case is less than 20% higher than the maximum heating value for the nominal reentry case. The highest maximum heating ratio occurred for the 5°, top surface, $Re_L = 5.6 \times 10^6$ case. The lowest maximum heating ratios occurred on the side surfaces at station B. This wind tunnel data analysis supports the 1.2 factor of safety on the heat transfer coefficient used in the JHU/APL thermal analysis that was done for a nominal 0° total angle-of-attack reentry.

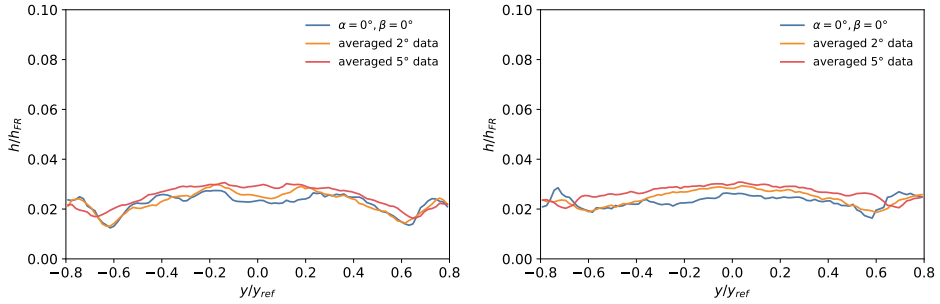

(a) Top Surface, Station A

(b) Top Surface, Station B

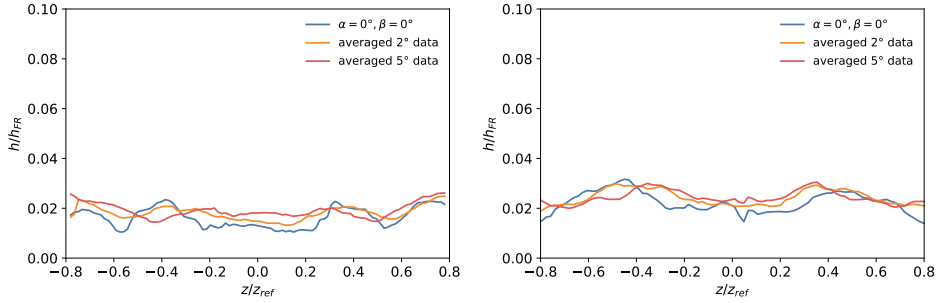

(c) Side Surface, Station A

(d) Side Surface, Station B

Fig. 14 Off-nominal and nominal TSM heating comparison for $Re_L = 2.9 \times 10^6$.

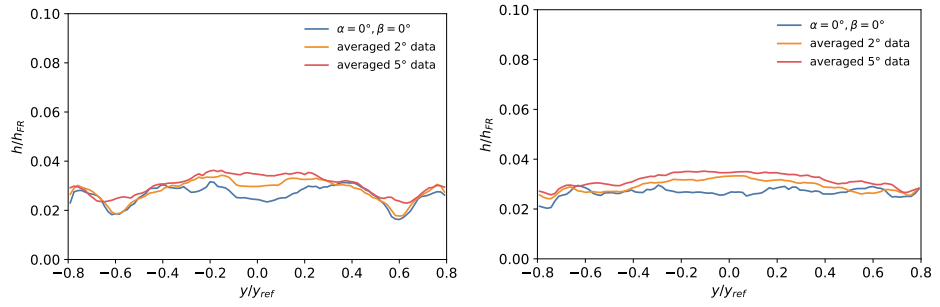

(a) Top Surface, Station A

(b) Top Surface, Station B

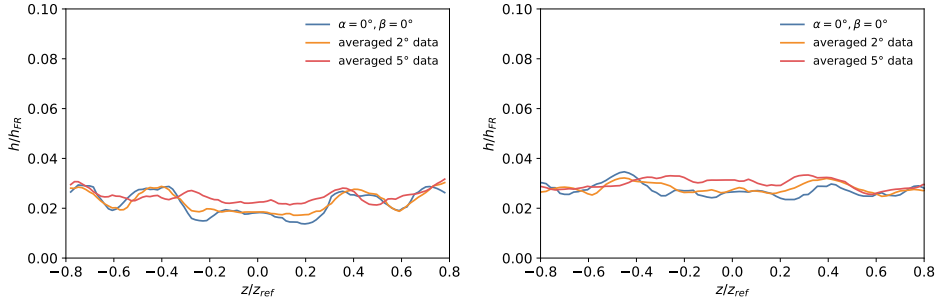

(c) Side Surface, Station A

(d) Side Surface, Station B

Fig. 15 Off-nominal and nominal TSM heating comparison for $Re_L = 5.6 \times 10^6$.

V. Summary

Aeroheating measurements of the BOLT aerodynamic fairings and TSM were made in the 20-Inch Mach 6 Air Tunnel at the NASA Langley Research Center. Aerodynamic fairings were deemed necessary on the BOLT Flight Research Vehicle, and there was concern about localized heating aft of the fairings on the TSM due to flow reattachment. A quick turnaround aeroheating wind tunnel test of the BOLT Flight Geometry, fairings, and TSM ahead of the BOLT CDR was requested. The model geometry was finalized four weeks ahead of the BOLT CDR, and a cast-ceramic model was fabricated and tested in the 20-Inch Mach 6 Air Tunnel using the global phoshor thermography technique. Preliminary global heating distributions on the fairings and TSM at a range of model attitudes were presented at the CDR. A subset of the global heating distributions on the BOLT Flight Geometry, fairings, and TSM were presented in this paper along with comparison to CFD predictions and an analysis of heating on the TSM region of the model.

The global heating distributions showed low heating on the fairings and low heating on the TSM as compared to the BOLT Flight Geometry surface. TSM heating increased with increasing Re_L and on the windward side of the vehicle with increasing angle-of-attack. Asymmetric TSM heating occurred on the top surface with changes in model β and on the side surface with changes in model α. Heating extracted at two axial stations on the TSM for the nominal vehicle reentry case (0° total angle-of-attack) was compared with heating for two off-nominal vehicle reentry cases (2° and 5° total angle-of-attack). The maximum heating for the off-nominal reentry cases considered were found to be less than 20% higher than the maximum heating for the nominal reentry case. These data support the JHU/APL thermal analysis of the TSM, which employed a 1.2 factor of safety on the heat transfer coefficient for the 0° total angle-of-attack case along with other conservative assumptions. Based on thermal analysis and wind tunnel test results, it was decided by the BOLT team that thermal protection was not necessary on the TSM.

Acknowledgments

Funding for the NASA Langley Research Center contributions to the BOLT project has been provided by the Hypersonics Technology Project. Dr. Bradley Wheaton at JHU/APL provided details of the BOLT TSM thermal analysis and provided guidance for TSM heating results presented in this paper. Model fabrication was completed by Robert Andrews and Michael Powers. Support for this test was provided by the NASA Langley 20-Inch Mach 6 Air Tunnel facility technicians and engineers: Johnny Ellis, Kevin Hollingsworth, and Larson Stacy.

References

[1] Wheaton, B. M., Berridge, D. C., Wolf, T. D., Stevens, R. T., and McGrath, B. E., "Boundary Layer Transition (BOLT) Flight Experiment Overview," AIAA 2018-2892, Jun. 2018. doi:10.2514/6.2018-2892.

[2] Berry, S. A., Mason, M. L., Greene, F. A., King, R. A., Rieken, E. F., and Basore, K. D., "LaRC Aerothermodynamic Ground Tests in Support of BOLT Flight Experiment," AIAA 2019-0091, Jan. 2019. doi:10.2514/6.2019-0091.

[3] Berger, K. T., Rufer, S. J., Hollingsworth, K. E., and Wright, S. A., "NASA Langley Aerothermodynamics Laboratory: Hypersonic Testing Capabilities," AIAA 2015-1337, Jan. 2015. doi:10.2514/6.2015-1337.

[4] Buck, G. M., "Rapid Model Fabrication and Testing for Aerospace Vehicles," AIAA 2000-0826, Jan. 2000. doi:10.2514/6.2000-826.

[5] Merski, N. R., "Global Aeroheating Wind-Tunnel Measurements Using Improved Two-Color Phosphor Thermography Method," *Journal of Spacecraft and Rockets*, Vol. 36, No. 2, 1999, pp. 160–170. doi:10.2514/2.3446.

[6] Buck, G. M., "Surface Temperature/Heat Transfer Measurement Using a Quantitative Phosphor Thermography System," AIAA 91-0064, Jan. 1991. doi:10.2514/6.1991-64.

[7] Mason, M. L. and Rufer, S. J., "Features of the Upgraded Imaging for Hypersonic Experimental Aeroheating Testing (IHEAT) Software," AIAA 2016-4322, Jun. 2016. doi:10.2514/6.2016-4322.

[8] Gnoffo, P. A., "An Upwind-Biased, Point-Implicit Relaxation Algorithm for Viscous, Compressible Perfect-Gas Flows," NASA TP-2953, Feb. 1990.

[9] Mazaheri, A., Gnoffo, P. A., Johnston, C. O., and Kleb, W. L., "LAURA Users Manual: 5.5-64987," NASA TM-2013-217800, Feb. 2013.

[10] Cheatwood, F. M. and Thompson, R. A., "The Addition of Algebraic Turbulence Modeling to Program LAURA," NASA TM-107758, Apr. 1993.

[11] Berridge, D. C., McKiernan, G., Wadhams, T. P., Holden, M., Wheaton, B. M., Wolf, T. D., and Schneider, S. P., "Hypersonic Ground Tests In Support of the Boundary Layer Transition (BOLT) Flight Experiment," AIAA 2018-2893, Jun. 2018. doi:10.2514/6.2018-2893.

[12] Berridge, D. C., Kostak, H. E., McKiernan, G. R., Wheaton, B. M., Wolf, T. D., and Schneider, S. P., "Hypersonic Ground Tests With High-Frequency Instrumentation In Support of the Boundary Layer Transition (BOLT) Flight Experiment," AIAA 2019-0090, Jan. 2019. doi:10.2514/6.2019-0090.

[13] Kostak, H. E., Bowersox, R. D., McKiernan, G. R., Thome, J., Candler, G. V., and King, R. A., "Freestream Disturbance Effects on Boundary Layer Instability and Transition on the AFOSR BOLT Geometry," AIAA 2019-0088, Jan. 2019. doi:10.2514/6.2019-0088.